

# Hole spin g-factor in p-type silicon single and double quantum dots

Henan Wei<sup>1</sup>, Seiya Mizoguchi<sup>1</sup>, Raisei Mizokuchi<sup>1</sup> and Tetsuo Kodera<sup>1</sup>

<sup>1</sup> Tokyo Institute of Technology  
2-12-1-S3-702, Okayama, Meguro-ku  
Tokyo 152-8552, Japan  
Phone: +81-3-5734-3421 E-mail: wei.h.ab@m.titech.ac.jp

## Abstract

This work demonstrates the detection and investigation of spin-related transport in physically defined silicon single and double quantum dots (QDs) fabricated on (110) silicon-on-insulator substrate. Landé g-factors in single QD and double QD are estimated respectively from observed magnetic field dependence characteristics. The g-factor of single QD is extracted as  $\sim 3$  from change of Coulomb diamond under different magnetic field conditions and that of double QD is calculated as  $\sim 2$  from change on Pauli spin blockade regions due to change of Zeeman energy. The difference on single QD and double QD is likely due to spin-orbit coupling.

## 1. Introduction

Holes confined in p-type silicon quantum dot (QD) have p-like wave functions, hence, have small hyperfine interaction and longer coherence time [1]. In comparison with electron spins, hole-spin-based QDs do not need additional structure to implement spin manipulation thanks to relatively strong spin-orbit coupling (SOC). Local magnetic field generated by SOC plays a role of a slanting magnetic field. Achievements on electrical hole spin manipulation by applying oscillating electric field have been reported in various devices with strong SOC [2]. To realize faster spin rotation within coherence time, hole-spin with stronger SOC is required. Mixing between heavy hole and light hole in (110) silicon are expected to generate a large SOC [3].

To achieve electrical spin manipulation via SOC, g-factor is estimated to characterize condition of spin resonance. In this work, g-factors of hole in (110) silicon are estimated in physically-defined p-type silicon single and double QDs.

## 2. Results and discussion

### 2.1 Device structure

In this work, physically-defined single and double QDs are fabricated in a metal-oxide-semiconductor (MOS) structure with undoped silicon-on-insulator (SOI) substrate grown on (110) surface. Fabrication process is technically similar with conventional MOS technology, hence, provides potential for large-scale quantum computing device architectures.

Fig. 1 shows a schematic of device structure with scanning electron microscopy (SEM) image focused on QD area. QDs are physically defined with etched structure and require no electrical gates to form a confinement potential barrier. Inter-dot coupling and accumulation of carriers can be adjusted by top gate structure. Side gates can be used to tune the en-

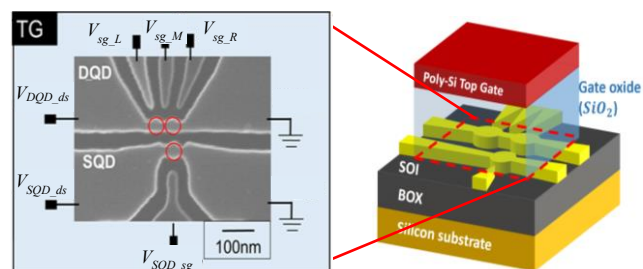


Fig.1 A schematic of device structure with SEM image focused on QD area.

ergy level of QDs electrically. The simple structure is promising for integration of qubits in the future.

### 2.2 g-factor estimation of single quantum dot

At 4.2 K, as shown in Fig. 2, by sweeping gate voltage and bias voltage, observed current through single QD shows white region in a diamond-like shape indicating uncondensed area resulted from discrete charging energy. This result is called Coulomb diamond and is peculiar to a single QD.

When applying different magnetic fields perpendicular to the substrate, the derivative of current through single QD is numerically derived as shown in Fig. 3. The energy state of hole spin splits into a ground state and an excited state with an energy difference known as Zeeman splitting  $E_Z$  given by  $E_Z = g\mu_B B$  where  $\mu_B$  denotes Bohr magneton,  $B$  denotes magnetic field.

Conductance peak appears around boundary of Coulomb diamond under zero magnetic field. When 2 T magnetic field is applied, expansion of conducting peak indicates that not only the ground state but also the excited state are within the transport window [4]. From change of width of conducted area which refers to change of Zeeman energy, perpendicular g-factor is estimated to be  $\sim 3$ .

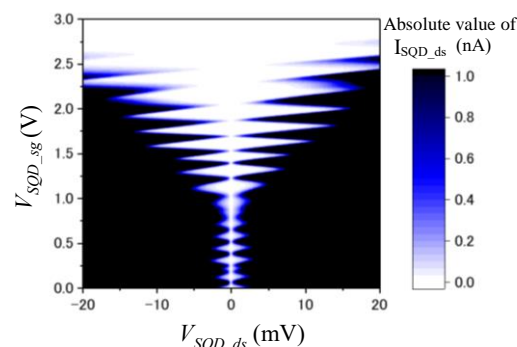


Fig. 2 Charge stability diagram of single QD at 4.2 K.

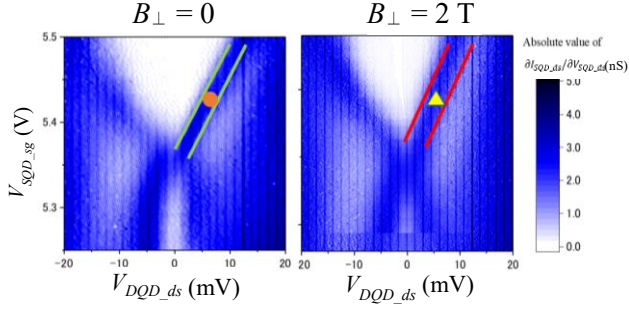


Fig. 3 Coulomb diamonds without and with out-of-plane magnetic field  $B_{\perp} = 2$  T. Orange circle in the left figure and yellow triangle in the right figure indicate widths of conducting area at the boundary of Coulomb diamond for both conditions, respectively. The width increases because of Zeeman splitting.

### 2.3 g-factor estimation of double quantum dot

In comparison with the method of estimating g-factor of single QD, dependence against magnetic field of current through a double QD is investigated.

In double QD systems, there can be two types of eigenstates referred to as the singlet and the triplet spin states. If a triplet state is formed, then the hole transport can be blocked by Pauli exclusion principle. This fundamental spin-dependent phenomenon is known as Pauli spin blockade (PSB) [5].

Fig 4(a) shows the triple points of double QD in a PSB regime at 260 mK under different magnetic fields. At the bottom of triple points, current is suppressed by PSB. By applying in-plane magnetic field, blockade area narrows down, indicating decreasing energy difference between singlet and triplet due to increasing Zeeman energy, from which parallel g-factor can be estimated as  $\sim 2$ .

Voisin et al. (Ref [6]) have demonstrated g-factor's anisotropy against magnetic field resulted from SOC in (100) silicon using a single QD. The g-factor obtained in this work is comparable with those of other silicon double QDs in similar structure. The reason why g-factor varies in different QDs is believed to be attributed to g-factor's anisotropy caused by the nature of hole [6] and by SOC. One can further conclude that larger out-of-plane g-factor than that of heavy hole ( $\sim 2.4$ ) is likely to be caused by large SOC of holes in (110) silicon.

When finite magnetic field is applied, SOC causes spin relaxation, resulting in transition from triplet to singlet [7]. The in-plane magnetic field dependence of the current in PSB area is measured to investigate spin relaxation characteristic via phonon assisted SOC as shown in Fig. 4(b).

Under low magnetic field, small leakage current can be resulted from the suppression of the spin relaxation due to van Vleck cancellation. With increasing of magnetic field, SOC induces partially lift of PSB and reveals a dip shape in the current. Leakage current can be fitted by a Lorentzian function [7] as represented below with dip width  $B_C$ , background current  $I_b$  and dip height  $I_{max}$ .

$$I(B) = I_{max} \left( 1 - \frac{8}{9} \frac{B_C^2}{B^2 + B_C^2} \right) + I_b \quad (1)$$

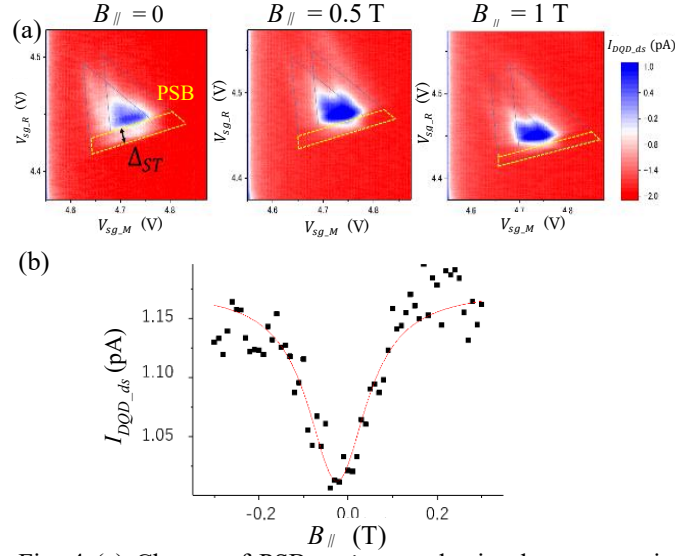


Fig. 4 (a) Change of PSB regions under in-plane magnetic field  $B_{\parallel} = 0, 0.5$  T and 1 T at 260 mK. (b) Magnetic field dependence of leakage current in PSB region fitted to a Lorentzian line shape.

There are many elements that cause lift of PSB, such as SOC, spin-flip cotunneling, and influence of nuclear spin. We can rule out latter two mechanisms and conclude that SOC dominates in the leakage current because of less nuclear spin in silicon [8,9] and absence of peak resulted from spin-flip cotunneling [10].

Based on the obtained g-factor, matching relationship between RF frequency and magnetic field of achieving hole spin resonance can be obtained from  $hf = g\mu_B B$  where  $h$  denotes Planck constant,  $f$  denotes frequency of applied RF signal. It hence provides possibilities towards electrical spin manipulation.

### 3. Conclusions

In this work, g-factors of single QD and double QD are estimated. Moreover, magnetic field dependence of leak current at PSB reveals strong SOC of hole in (110) silicon. With referring to estimated g-factor of double QD, electric dipole spin resonance via the strong SOC is expected to be implemented to achieve further spin-based qubit manipulations.

### Acknowledgements

This study was financially supported by JST CREST (JPMJCR 1675) and MEXT Q-LEAP.

### References

- [1] Y. Yamaoka et al 2017 Jpn. J. Appl. Phys. 56 04CK07
- [2] V. S. Pribiag, et al., Nat. Nanotechnol. 8, 170 (2013).
- [3] K. Suzuki, and J. C. Hensel, *Physical Review B* 9 4184 (1974)
- [4] M. Brauns et al., Phys. Rev. B, 93, 121408(R) (2016)
- [5] K. Ono, et al., Science 297, 1313 (2002).
- [6] B. Voisin, et al., Nano Lett. 16 (1), 88 (2016).
- [7] J. Danon and Y. V. Nazarov, Phys. Rev. B **80**, 041301 (2009).
- [8] M. Veldhorst, et al., Nature 526, 410 (2015).
- [9] X. Hao, et al., Nat. Commun. 5, 3860 (2014).
- [10] G. Yamahata, et al., Phys. Rev. B 86, 115322 (2012).